Available online at www.sciencedirect.com
SCIENCE DIRECT®
Journal of Organometallic Chemistry 665 (2003) 176–185
Journal of Organometallic Chemistry
www.elsevier.com/locate/jorganchem

Supported organometallic complexes Part XXXV. Synthesis, characterization, and catalytic application of a new family of diamine(diphosphine)ruthenium(II) complexes☆

Ekkehard Lindner *, Hermann A. Mayer *, Ismail Warad, Klaus Eichele

Institut für Anorganische Chemie der Universität Tübingen, Auf der Morgenstelle 18, D-72076 Tübingen, Germany

Received 24 July 2002; accepted 30 October 2002

Abstract

The novel diamine(dppp)ruthenium(II) complexes $\mathbf{3L_1}$–$\mathbf{3L_{12}}$ have been obtained by reaction of equimolar amounts of $Cl_2Ru(dppp)_2$ **(2)** with the diamines $\mathbf{L_1}$–$\mathbf{L_{12}}$ in excellent yields. Within a few minutes one of the diphosphine ligands was quantitatively exchanged by the corresponding diamine. X-ray structural investigations of $\mathbf{3L_1}$, $\mathbf{3L_2}$, and $\mathbf{3L_8}$ show triclinic unit cells with the space groups $P\bar{1}$ ($\mathbf{3L_1}$, $\mathbf{3L_2}$) and P 1 ($\mathbf{3L_8}$). Whereas in solution all these complexes prefer a *trans*-$RuCl_2$ configuration, in the solid state *cis*-($\mathbf{3L_1}$, $\mathbf{3L_2}$) and *trans*-isomers ($\mathbf{3L_8}$) were observed. With the exception of $\mathbf{3L_5}$, $\mathbf{3L_6}$, and $\mathbf{3L_{12}}$ all mentioned ruthenium complexes are highly catalytically active in the hydrogenation of the α,β-unsaturated ketone *trans*-4-phenyl-3-butene-2-one. In most cases the conversions and selectivities toward the formation of the unsaturated alcohol *trans*-4-phenyl-3-butene-2-ol were >99% with high turnover frequencies (TOFs) under mild conditions.

Keywords: Ruthenium(II) complexes; Crystal structures; Diphos ligand; Diamine ligands; Catalytic hydrogenation

1. Introduction

The hydrogenation of carbonyl compounds to alcohols is among the most applied processes in organic chemistry [2–5]. Recently Noyori et al. discovered a ruthenium(II) complex system containing diphosphine and 1,2-diamine ligands which, in the presence of a base and 2-propanol, proved to be excellent catalysts for the hydrogenation of ketones under mild conditions [6–8]. Subsequently chiral ruthenium(II) complexes were developed for the asymmetric hydrogenation of functionalized ketones [8–12]. If these complexes are supported no leaching takes place and the activity and enantioselectiveity remained constant even after twelve runs [11]. A mechanism of this reaction has been suggested [7,10,13,14]. The source of the transferred hydrogen atom was attributed to a metal-centered hydride. Generally, the most widely accepted theory is that at least one NH and a RuH unit is intimately involved in the hydride transfer process [8,13]. It has been considered that the catalytic activity is traced back to the electronic properties of the coordination center and that the stereoselectivity is controlled by the chiral ligand [13]. Similar catalyst systems were established by Burk, Bergens, and Morris et al. [15–18]. In the last mentioned case the authors used mono- and dihydride(diamine)(diphos)ruthenium(II) complexes and found that in the absence of a base no hydrogenation of the carbonyl group has taken place [17].

In a recent work we reported on the preparation of novel diamineruthenium(II) complexes which were provided with hemilabile ether–phosphine ligands [1,19]. These complexes proved to be excellent catalysts in the hydrogenation of α,β-unsaturated ketones [1]. By the introduction of T-silyl functions into the ether–phosphine ligands, these complexes can be supported to a polysiloxane matrix after a sol–gel process [20]. Now we introduce a facile and fast synthesis of a series of diamine(diphos)ruthenium(II) complexes. As a diphos

☆ For Part XXXIV see Ref. [Inorg. Chim. Acta (in press)].

* Corresponding authors. Tel.: +49-7071-29-72039; fax: +49-7071-29-5306

E-mail addresses: ekkehard.lindner@uni-tuebingen.de (E. Lindner), hermann.mayer@uni-tuebingen.de (H.A. Mayer).

0022-328X/02/$ - see front matter © 2002 Elsevier Science B.V. All rights reserved.
PII: S0022-328X(02)02112-5

ligand 1,3-bis(diphenylphosphino)propane was selected, because in a subsequent investigation it can be attached to a spacer unit at the symmetric carbon atom 2 of the ligand backbone [21,22]. Three complexes (**3L$_1$**, **3L$_2$**, and **3L$_8$**) were subjected to an X-ray structural investigation. Most of the complexes are highly active in the catalytic hydrogenation of *trans*-4-phenyl-3-butene-2-one.

2. Results and discussion

2.1. Synthesis of the diamine[bis(diphenylphosphino)propane]ruthenium(II) complexes 3L$_1$–3L$_{12}$

The precursor compound *trans*-$Cl_2Ru(dppp)_2$ (**2**) was obtained by a substitution reaction starting from $Cl_2Ru(PPh_3)_3$ (**1**) and dppp in dichloromethane [23]. If **2** is treated with the diamines **L$_1$**–**L$_{12}$** in dichloromethane, the yellow, somewhat air-insensitive mixed diamine[bis(diphenylphosphino)propane]ruthenium(II) complexes **3L$_1$**–**3L$_{12}$** were formed in good to excellent yields. Even in the presence of excess diamine only one dppp ligand was exchanged (Scheme 1). The yields of the complexes **3L$_1$**–**3L$_{12}$** depend on steric factors of the diamine ligands. If one or both hydrogen atoms at the nitrogen donors are replaced by alkyl or aryl groups no reaction takes place. Bipyridine and other aromatic *N*-derivatives do not react with complex **2,** even under elevated conditions. Complexes **3L$_1$**–**3L$_{12}$** are soluble in chlorinated organic solvents and insoluble in ethers and aliphatic hydrocarbons. Their molecular composition was corroborated by FAB mass spectra.

2.2. NMR and IR spectroscopic investigations

In the ^{1}H-NMR spectra of the diamine(dppp)ruthenium(II) complexes **3L$_1$**–**3L$_{12}$** characteristic sets of

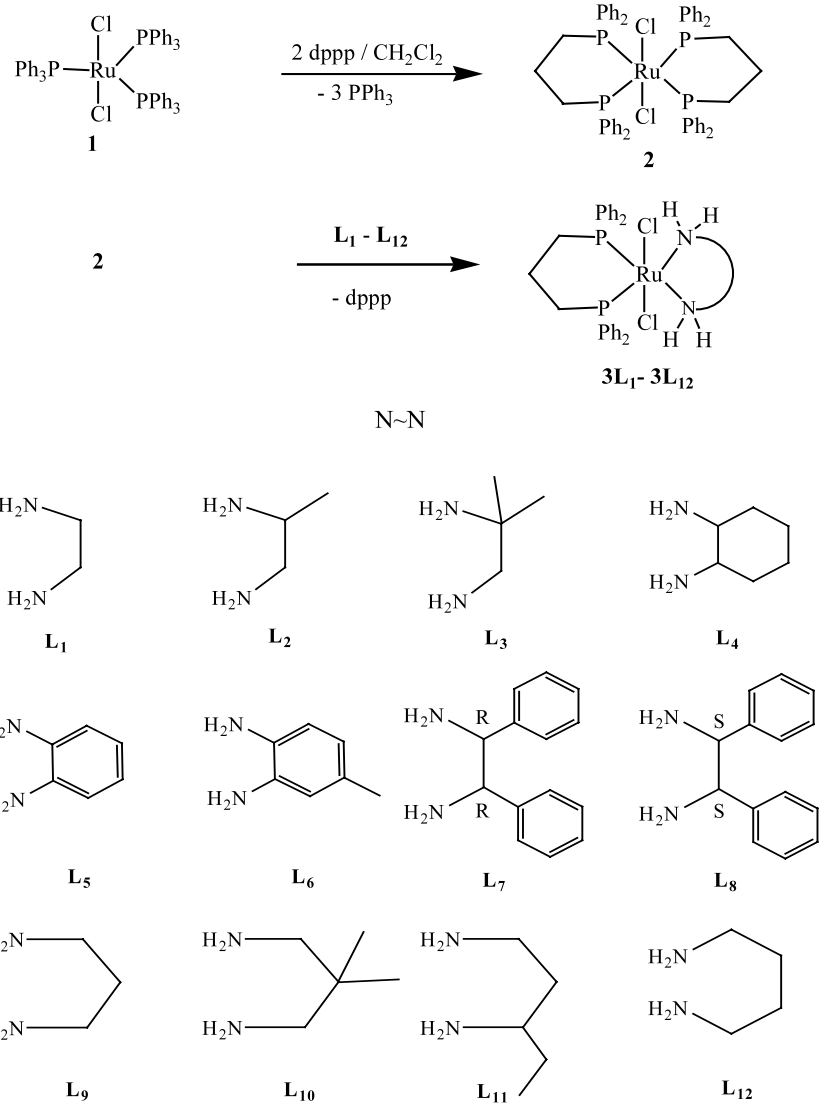

Scheme 1.

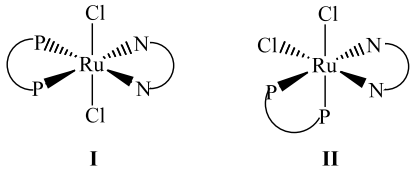

Chart 1.

signals were observed, which are attributed to the phosphine and diamine ligands. Their assignment was supported by two-dimensional H,H-COSY experiments, which establish the connectivity between NH_2 and CH_2 functions in the diamine ligands, as well as between CH_2 and CH_2P groups in the phosphine fragments. The integration of the ^1H resonances confirm that the phosphine to diamine ratios are in agreement with the compositions of **3L$_1$**–**3L$_{12}$**. Because singlets are observed in the $^{31}P\{^1H\}$-NMR spectra of the $RuCl_2$(dppp)diamine complexes **3L$_1$**, **3L$_4$**, **3L$_5$**, **3L$_7$**–**3L$_{10}$**, and **3L$_{12}$** the C_1 symmetric structure **II** in Chart 1 is ruled out. In the cases of **3L$_2$**, **3L$_3$**, and **3L$_{11}$** the asymmetric diamines cause a loss of the C_2-axis which results in a splitting of the ^{31}P resonances into AB patterns. However, in **3L$_6$** this asymmetry is too remote from the phosphorus atoms to generate an observable splitting of the $^{31}P\{^1H\}$-NMR signal. The ^{31}P chemical shifts and the ^{31}P–^{31}P coupling constants are consistent with a *cis* arrangement of the P groups according to structure **I** (Chart 1).

Characteristic sets of resonances between 15–30 and 35–49 ppm are found in the $^{13}C\{^1H\}$-NMR spectra of **3L$_1$**–**3L$_{12}$**, which are attributed to the aliphatic part of the phosphine and diamine ligands, respectively. AXX′ splitting patterns were observed for the aliphatic and aromatic carbon atoms directly attached to phosphorus. They are caused by the interaction of the magnetically inequivalent phosphorus atoms with the ^{13}C nuclei. This pattern is also consistent with structure **I** (Chart 1).

The IR spectra of the complexes **3L$_1$**–**3L$_{12}$** in particular show four sets of characteristic absorptions in the ranges 3336–3319, 3268–3215, 3178–3165, and 275–254 cm^{-1}, which can be assigned to NH_2, amine–CH, phosphine–CH and RuCl stretching vibrations, respectively.

2.3. X-ray structural determination of 3L$_1$, 3L$_2$, and 3L$_8$

Crystals suitable for X-ray structural analysis have been obtained for complexes **3L$_1$**, **3L$_2$**, and **3L$_8$**. Their molecular structures are shown in Fig. 1 and selected bond distances, bond angles, and torsion angles are listed in Table 1. All three compounds feature two different chelate systems: a six-membered bis(phosphine) ring that is common to all three and adopts a similar chair conformations in each case, and a five-membered diamine ring that differs from complex to complex only in the number and kind of substituents at the carbon backbone. While the bis(phosphine) ring allows for P–Ru–P angles very close to the ideal value of 90°, the smaller diamine enforces N–Ru–N angles that are 9–13° less than the ideal value. The most striking difference between the three complexes is the finding that **3L$_1$** and **3L$_2$** form the *cis*-chloro isomer **II** (Chart 1), while **3L$_8$** crystallizes as the more usual *trans*-chloro isomer **I**, although all three compounds were shown by spectroscopic methods to be the *trans*-chloro isomer in solution (vide supra).

The structure of **3L$_1$** is similar to that of a bis(ether–phosphine)ruthenium complexes, (en)($H_3COCH_2CH_2P$-Ph_2)$_2RuCl_2$, described earlier [19]: the Ru–P and Ru–N distances *trans* to chlorine are slightly shorter than those *trans* to nitrogen or phosphorus, respectively. Similarly, the Ru–Cl distances *trans* to nitrogen are slightly shorter than those *trans* to phosphorus. The diamine chelate prefers the twist conformation, with C(28) 0.24 Å below and C(29) 0.42 Å above the N(1)–Ru(1)–N(2) plane. Fig. 1 and the data in Table 1 indicate that the structure of **3L$_2$** is quite similar to that of **3L$_1$**, albeit the former cocrystallizes with one molecule of dichloromethane. It appears that, otherwise, the methyl substituent at C(28) exerts little effect on the stuctural parameters, although the twist conformation of the diamine is more regular, with C(28) and C(29) displaced by −0.32 and 0.33 Å below and above the N(1)–Ru(1)–N(2) plane. In contrast, the phenyl substituents of the diamine in **3L$_8$** cause a change in the symmetry of the complex: **3L$_8$** crystallizes as the *trans*-chloro isomer with two independent molecules in the asymmetric unit. Both molecules are arranged about a pseudo-inversion center that approximately maps the greater part of molecule A to molecule B, except for the *S,S*-configuration of the diamine ligand that does not allow for a centrosymmetric space group. In addition, the diamine chelates adopt slightly different conformations: in molecule B it is the normal twist conformation, with C(28B) and C(29B) by 0.31 and −0.50 Å above and below the N–Ru–N plane, but in A it is close to an envelope with C(29A) at the top: C(28A) and C(29A) are displaced by −0.07 and 0.59 Å from the N–Ru–N plane.

2.4. Catalytic activity of the ruthenium(II) complexes 3L$_1$–3L$_{12}$ in the hydrogenation of trans-4-phenyl-3-butene-2-one

To study the catalytic activity of the ruthenium(II) complexes **3L$_1$**–**3L$_{12}$**, *trans*-4-phenyl-3-butene-2-one was selected as a model substrate for different reasons: (i) the hydrogenation of α,β-unsaturated ketones is not that easy, because of the conformational flexibility of the substrates [2]; (ii) the ketone reveals UV activity, which disappears upon hydrogenation of the ketone due to interruption of the conjugation. This effect can be

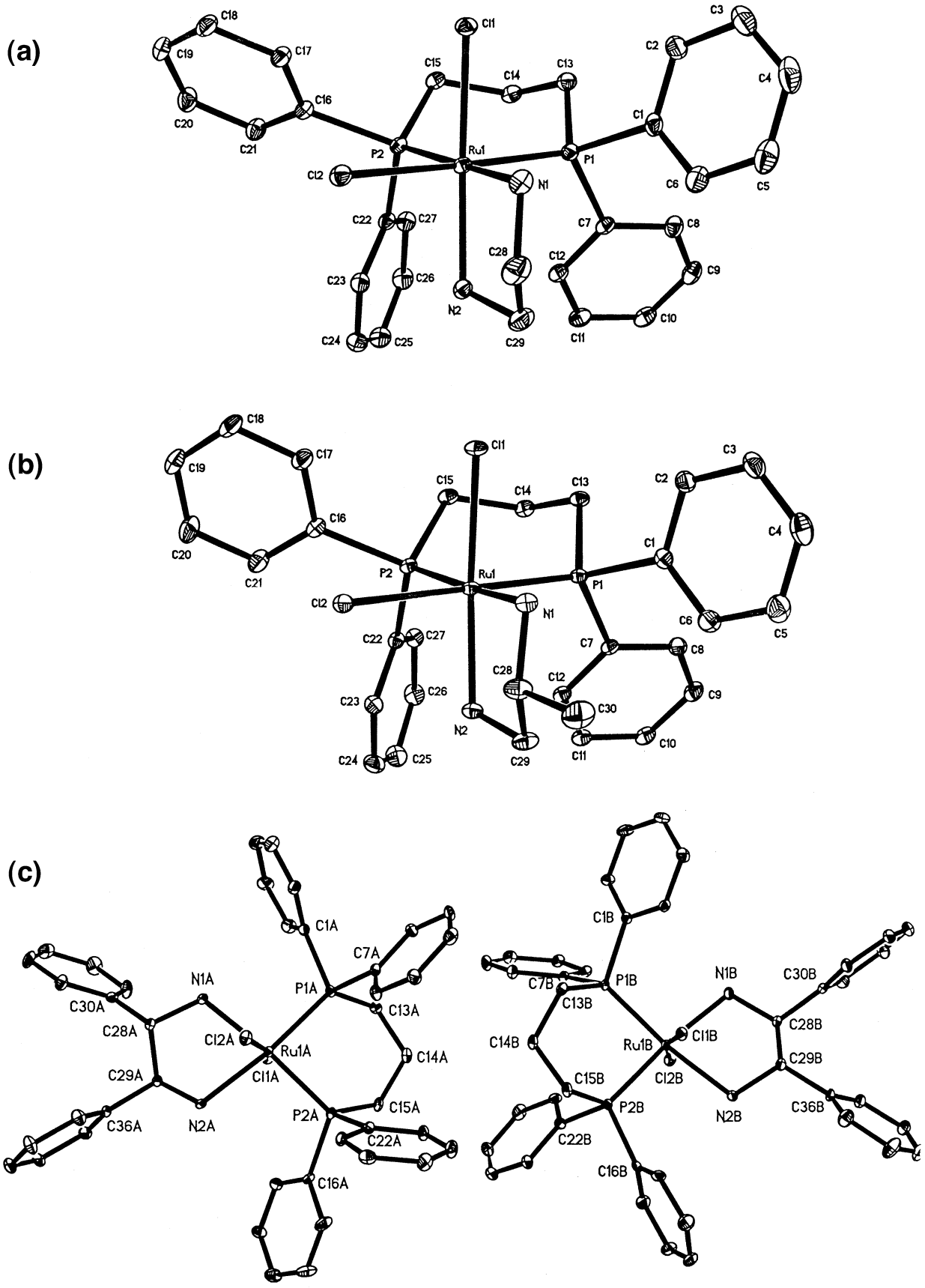

Fig. 1. ORTEP plots of $\mathbf{3L_1}$ (a), $\mathbf{3L_2}$ (b) and the two crystallographically nonequivalent molecules of $\mathbf{3L_8}$ (c) with atom labeling scheme. Thermal ellipsoids are drawn at the 20% probability level, hydrogens and solvent molecules are omitted for clarity.

Table 1
Selected bond lengths (Å) and bond and torsion angles (°) for **3L$_1$**, **3L$_2$**, and molecules A and B of **3L$_8$**

	3L$_1$	**3L$_2$**	**3L$_8$**, A	**3L$_8$**, B
Bond lengths				
Ru(1)–Cl(1)	2.404(2)	2.4208(8)	2.4293(10)	2.4227(11)
Ru(1)–Cl(2)	2.466(2)	2.5103(10)	2.4164(11)	2.4122(11)
Ru(1)–P(1)	2.2321(18)	2.2440(10)	2.2563(12)	2.2640(12)
Ru(1)–P(2)	2.2820(14)	2.2769(8)	2.2652(12)	2.2518(12)
Ru(1)–N(1)	2.172(2)	2.1629(19)	2.171(4)	2.183(4)
Ru(1)–N(2)	2.147(3)	2.1333(18)	2.172(4)	2.193(4)
Bond angles				
Cl(1)–Ru(1)–Cl(2)	89.13(9)	91.98(3)	165.80(4)	167.15(4)
P(1)–Ru(1)–P(2)	91.67(6)	90.88(3)	89.21(4)	89.35(4)
N(1)–Ru(1)–N(2)	80.80(10)	79.87(7)	78.07(14)	77.28(14)
N(1)–Ru(1)–Cl(1)	86.11(8)	84.71(6)	83.75(11)	87.97(11)
N(2)–Ru(1)–Cl(1)	166.24(6)	164.14(5)	89.23(10)	83.99(11)
P(1)–Ru(1)–Cl(1)	87.89(9)	87.94(3)	88.53(4)	89.78(4)
P(2)–Ru(1)–Cl(1)	91.48(5)	90.95(3)	90.70(4)	89.07(4)
N(1)–Ru(1)–Cl(2)	80.85(8)	83.24(6)	83.07(11)	84.19(11)
N(2)–Ru(1)–Cl(2)	84.66(10)	82.62(6)	82.89(10)	84.37(11)
P(1)–Ru(1)–Cl(2)	174.25(2)	177.88(2)	98.04(4)	101.25(4)
P(2)–Ru(1)–Cl(2)	93.32(6)	91.24(3)	101.91(4)	97.54(4)
Torsion angles				
P(2)–Ru(1)–P(1)–C(13)	40.48(10)	44.08(9)	49.65(16)	46.73(16)
Ru(1)–P(1)–C(13)–C(14)	−61.45(18)	−63.64(16)	−65.1(3)	−50.41(17)
P(1)–C(13)–C(14)–C(15)	72.2(2)	71.1(2)	68.6(4)	65.1(5)
C(13)–C(14)–C(15)–P(2)	−69.4(3)	−68.3(2)	−67.0(5)	−68.3(5)
C(14)–C(15)–P(2)–Ru(1)	55.51(19)	55.55(18)	59.9(3)	66.3(4)
C(15)–P(2)–Ru(1)–P(1)	−38.22(10)	−39.71(8)	−46.34(17)	−50.41(17)
N(2)–Ru(1)–N(1)–C(28)	−10.06(18)	−13.47(16)	2.8(2)	13.1(2)
Ru(1)–N(1)–C(28)–C(29)	35.2(3)	37.6(3)	−28.7(3)	−43.9(3)
N(1)–C(28)–C(29)–N(2)	−52.1(3)	−50.8(3)	49.0(3)	61.5(3)
C(28)–C(29)–N(2)–Ru(1)	41.9(3)	38.9(2)	−47.3(3)	−50.3(3)
C(29)–N(2)–Ru(1)–N(1)	−17.43(17)	−13.88(16)	24.9(2)	20.7(2)

used to carry out kinetic investigations [24]; (iii) the chosen ketone allows to study the selectivity of the catalysts. Three different possibilities of the hydrogenation process are to be expected (Scheme 2). The selective hydrogenation of the carbonyl function affords the corresponding unsaturated alcohol *trans*-4-phenyl-3-butene-2-ol **A**, which is the most desired product. Unwanted and hence of minor interest is the hydrogenation of the C=C double bond, leading to the saturated ketone **B**. Also not in the focus of our interest is the hydrogenation of both the C=O and C=C bonds, resulting in the formation of the saturated alcohol **C**. 2-Propanol served as a solvent, but the catalysts were only active in the presence of excess hydrogen and a cocatalyst (e.g. KOH). All hydrogenations were carried out under mild conditions at three bar H_2 pressure and 35 °C. Results are listed in Table 2.

As expected $RuCl_2(dppp)_2$ (**2**) was completely inactive in the hydrogenation of unsaturated ketones, which is traced back to the absence of the diamine. The starting complex $RuCl_2(PPh_3)_2$ (**1**) was only slightly active under the applied mild reaction conditions. However, the selectivity was low, because both the C=O and C=C functions were hydrogenated to give **C** with a conversion of only 28% (Table 2). With the exception of **3L$_5$**, **3L$_6$**, and **3L$_{12}$** all ruthenium(II) complexes (**3L$_1$**–**3L$_4$**, **3L$_7$**–**3L$_{11}$**) revealed high activity and excellent selectivity. In the case of **3L$_1$**, **3L$_4$**, **3L$_7$**–**3L$_9$**, and **3L$_{11}$**, a conversion of 100% has been achieved in less than 1 h, and the only product was **A** (Table 2). If one or two methyl groups are introduced into the backbone of 1,2-diamines, a

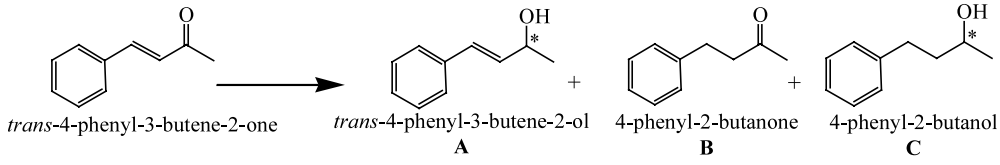

Scheme 2.

Table 2
Hydrogenation of *trans*-4-phenyl-3-butene-2-one [a]

Run	Catalyst	Conversion (%) [b]	TOF [c]	Selectivity (%) [b]		
				A	B	C
1	**1**	28 [d]	12	0	0	100
2	**2**	0 [d]	0	0	0	0
3	**3L$_1$**	100	1080	100	0	0
4	**3L$_2$**	90	776	100	0	0
5	**3L$_3$**	54	540	100	0	0
6	**3L$_4$**	100	1210	100	0	0
7	**3L$_5$**	28 [e]	18	0	0	100
8	**3L$_6$**	0 [d]	0	0	0	0
9	**3L$_7$**	100	1490	100	0	0
10	**3L$_8$**	100	1724	100	0	0
11	**3L$_9$**	100	926	100	0	0
12	**3L$_{10}$**	92	920	100	0	0
13	**3L$_{11}$**	100	2000	100	0	0
14	**3L$_{12}$**	25 [e]	17	45	0	55

[a] Reaction was conducted at 35 °C using 3–5 g of substrate ($S/C = 1000$) in 50 ml of 2-propanol, $P_{H_2} = 3$ bar, [Ru: KOH: Substrate][1:10:1000].
[b] Yields and selectivities were determined by GC.
[c] TOF: turnover frequency ($mol_{sub}\ mol_{cat}^{-1}\ h^{-1}$).
[d] Overnight reaction.
[e] 15 h reaction.

constant decrease of the turnover frequencies (TOFs) and the conversions was observed, which is probably due to steric effects (Table 2 and Fig. 2).

3. Conclusion

In this work a set of 12 (dppp)ruthenium(II) complexes with different aliphatic 1,2-, 1,3-, 1,4-, cycloaliphatic and aromatic 1,2-diamines as well as chiral aliphatic 1,2-diamines have been made accessible by a new method of fast ligand exchange. While in solution all these complexes prefer a *trans*-$RuCl_2$ configuration, in the solid state *cis*- and *trans*- isomers were formed. With exception of the complexes with aromatic diamines all other species were highly active catalysts in the hydrogenation of *trans*-PhCH=CHC(O)Me even under mild conditions. In most cases the selectivity was 100% toward the hydrogenation of only the carbonyl group. Interestingly complex **3L$_{11}$** with 1,3-diamine as a ligand was more active than 1,2-diamine complexes, which has never been observed.

4. Experimental

4.1. General remarks, materials, and instrumentations

All reactions were carried out in an inert atmosphere (argon) by using standard high vacuum and Schlenk-line techniques unless otherwise noted. Prior to use CH_2Cl_2, *n*-hexane, and Et_2O were distilled from CaH_2, $LiAlH_4$, and from sodium–benzophenone, respectively.

1,3-Bis(diphenylphosphino)propane (dppp) was prepared according to literature methods [25]. The diamines were purchased from Acros, Fluka, and Merck and had to be purified by distillation and recrystallization, respectively. Ph_3P, *n*-BuLi, and $RuCl_3 \cdot 3\ H_2O$ were available from Merck and ChemPur, respectively, and were used without further purification. Elemental analyses were carried out on an Elementar Varrio EL analyzer. High-resolution ^1H, $^{13}C\{^1H\}$, DEPT 135, and $^{31}P\{^1H\}$-NMR spectra were recorded on a Bruker DRX 250 spectrometer at 298 K. Frequencies are as follows: ^1H-NMR 250.12 MHz, $^{13}C\{^1H\}$-NMR 62.9 MHz, and $^{31}P\{^1H\}$-NMR 101.25 MHz. Chemical shifts in the ^1H and $^{13}C\{^1H\}$-NMR spectra were measured relative to partially deuterated solvent peaks which are reported relative to TMS. ^{31}P chemical shifts were measured relative to 85% H_3PO_4. IR data were obtained on a Bruker IFS 48 FTIR spectrometer. Mass spectra: EIMS, Finnigan TSQ70 (200 °C) and FABMS, Finnigan 711A (8 kV), modified by AMD and reported as mass/charge (m/z). The analyses of the hydrogenation experiments were performed on a GC 6000 Vega Gas 2 (Carlo Erba Instrument) with a FID and capillary column PS 255 [10 m, carrier gas, He (40 kPa), integrator 3390 A (Hewlett–Packard)].

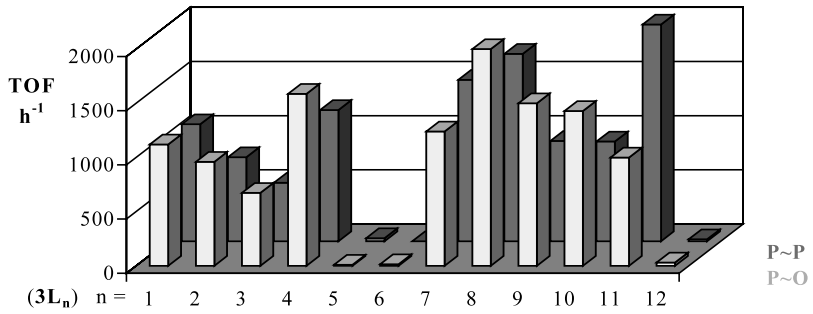

Fig. 2. Ruthenium-catalyzed hydrogenation of *trans*-4-phenyl-3-butene-2-one. P–P ≅ is $RuCl_2$(diphos)diamine, P–O ≅ $RuCl_2$(ether–phosphine)$_2$diamine [1]. Reaction conditions: 2-propanol, KOH as cocatalyst, $T = 35$ °C and $P_{H_2} = 3$ bar.

4.2. General procedure for the preparation of the complexes 3L1–3L12 (see Scheme 1)

The corresponding diamine (10% excess of $\mathbf{L_1}$–$\mathbf{L_{12}}$) was dissolved in 10 ml of dichloromethane and the solution was added dropwise to a stirred solution of **2** in 10 ml of dichloromethane within 5 min. The mixture was stirred for ca. 10–30 min at room temperature while the color changed from brown to yellow. After removal of any turbidity by filtration (P4), the volume of the solution was concentrated to about 5 ml under reduced pressure. Addition of 40 ml of diethyl ether caused precipitation of a solid, which was filtered (P4). After recrystallization from dichloromethane–*n*-hexane, the corresponding complexes were obtained in analytically pure form.

4.2.1. 3L1

Complex **2** (500 mg, 0.50 mmol) was treated with $\mathbf{L_1}$ (0.035 ml, 0.55 mmol) to give $\mathbf{3L_1}$. Yield 312 mg (97%) of a yellow powder, m.p. 310 °C (dec.). ^{1}H-NMR ($CDCl_3$): δ (ppm) 1.82 (m, 2H, CH_2), 2.74 (br, 12H, PCH_2, NH_2, NCH_2), 7.17–7.60 (m, 20H, C_6H_5). $^{31}P\{^1H\}$-NMR ($CDCl_3$): δ (ppm) 41.30. $^{13}C\{^1H\}$-NMR ($CDCl_3$): δ (ppm) 19.23 (s, CH_2), 26.1 (m [26]a, $N = 35.02$ Hz, PCH_2), 43.64 (s, NCH_2), 128.32 (m [26]b, $N = 8.08$ Hz, *m*-C_6H_5), 129.20 (s, *p*-C_6H_5), 133.13 (br, *o*-C_6H_5). FABMS; (*m*/*z*): 644.1 [M^+]. Anal. Found: C, 54.04; H, 5.32; Cl, 11.00; N, 4.35. Calc. for $C_{29}H_{34}Cl_2N_2P_2Ru$: C, 54.07; H, 5.16; Cl, 10.84; N, 4.19%.

4.2.2. 3L2

Complex **2** (500 mg, 0.50 mmol) was treated with $\mathbf{L_2}$ (0.048 ml, 0.55 mmol) to give $\mathbf{3L_2}$. Yield 302 mg (91%) of a yellow powder, m.p. 291 °C (dec.). ^{1}H-NMR ($CDCl_3$): δ (ppm) 0.92 (d, $^3J_{HH} = 6.28$ Hz, 3H, CH_3), 1.82 (m, 2H, CH_2), 2.30–2.90 (m, 10H, PCH_2, NH_2, NCH_2), 3.11 (m, 1H, NCH), 7.17–7.60 (m, 20H, C_6H_5). $^{31}P\{^1H\}$-NMR ($CDCl_3$): δ (ppm) 41.22, 42.13 (AB pattern, $^2J_{PP} = 52.20$ Hz). $^{13}C\{^1H\}$-NMR ($CDCl_3$): δ (ppm) 19.22 (s, CH_2), 20.53 (s, CH_3), 25.71 (d, $^1J_{PC} = 4.40$ Hz, PCH_2), 26.10 (d, $^1J_{PC} = 4.40$ Hz, PCH_2), 49.73 (s, NCH_2), 51.00 (s, NCH), 128.93 (m, *m*-C_6H_5), 131.21 (m, *p*-C_6H_5), 133.94 (m, *o*-C_6H_5), 137.55, 138.05 (m, *i*-C_6H_5) FABMS; (*m*/*z*): 658.1 [M^+]. Anal. Found: C, 54.97; H, 5.51; Cl, 10.77; N, 4.25. Calc. for $C_{30}H_{36}Cl_2N_2P_2Ru$: C, 55.26; H, 5.17; Cl, 10.91; N, 4.06%.

4.2.3. 3L3

Complex **2** (500 mg, 0.50 mmol) was treated with $\mathbf{L_3}$ (0.057 ml, 0.55 mmol) to give $\mathbf{3L_3}$. Yield 288 mg (85%) of a yellow powder, m.p. 302 °C (dec.). ^{1}H-NMR ($CDCl_3$): δ (ppm) 1.12 (s, 6H, CH_3), 1.80 (m, 2H, CH_2), 2.66–2.91 (br, 10H, PCH_2, NH_2, NCH_2), 7.14–7.63 (m, 20H, C_6H_5). $^{31}P\{^1H\}$-NMR ($CDCl_3$): δ (ppm) 41.59, 42.32 (AB pattern, $^2J_{PP} = 52.20$ Hz). $^{13}C\{^1H\}$-NMR ($CDCl_3$): δ (ppm) 19.44 (s, CH_2), 25.43 (dd, $^1J_{PC} = 4.4$, $^3J_{PC} = 4.4$ Hz, PCH_2) 25.74 (dd, $^1J_{PC} = 4.4$, $^3J_{PC} = 4.4$ Hz, PCH_2), 29.36 (s, CH_3), 53.17 (s, NC), 54.58 (s, NCH_2), 126.69 (m, *m*-C_6H_5), 127.75 (m, *p*-C_6H_5), 131.79 (m, *o*-C_6H_5), 136.44 (m, *i*-C_6H_5). FABMS; (*m*/*z*): 672.1 [M^+]. Found: C, 55.36; H, 5.69; Cl, 10.54; N, 4.17. Calc. for $C_{31}H_{38}Cl_2N_2P_2Ru$: C, 54.90; H, 5.33; Cl, 10.42; N, 4.11%.

4.2.4. 3L4

Complex **2** (500 mg, 0.50 mmol) was treated with $\mathbf{L_4}$ (0.060 g, 0.55 mmol) to give $\mathbf{3L_4}$. Yield 348 mg (99%) of a yellow–brown powder, m.p. 298 °C (dec.). ^{1}H-NMR ($CDCl_3$): δ (ppm) 0.88–2.14 (m, 10H, C_6H_{10}), 1.81 (m, 2H, CH_2), 2.49–2.81 (m, 8H, PCH_2, NH_2), 7.12–7.66 (m, 20H, C_6H_5). $^{31}P\{^1H\}$-NMR ($CDCl_3$): δ (ppm) 41.63. $^{13}C\{^1H\}$-NMR ($CDCl_3$): δ (ppm) 19.31 (s, CH_2), 24.96 (s, CH_2CH_2CH), 26.15 (m [26]a, $N = 35.02$ Hz, PCH_2), 36.39 (s, $NCHCH_2$), 57.62 (s, $NCHCH_2$), 128.16 (m, *m*-C_6H_5), 129.15 (m, *p*-C_6H_5), 133.11 (m, *o*-C_6H_5). FABMS; (*m*/*z*): 698.1 [M^+]. Anal. Found: C, 56.73; H, 5.77; Cl, 10.15; N, 4.01. Calc. for $C_{33}H_{40}Cl_2N_2P_2Ru$: C, 56.48; H, 5.76; Cl, 10.03; N, 4.07%.

4.2.5. 3L5

Complex **2** (500 mg, 0.50 mmol) was treated with $\mathbf{L_5}$ (0.06 g, 0.55 mmol) to give $\mathbf{3L_5}$. Yield 279 mg (81%) of a light brown powder, m.p. 303 °C (dec.). ^{1}H-NMR ($CDCl_3$): δ (ppm) 1.75 (m, 2H, CH_2), 2.67 (br, 4H, PCH_2), 4.13 (br, 4H, NH_2), 6.72–7.74 (m, 24H, C_6H_5, C_6H_3). $^{31}P\{^1H\}$-NMR ($CDCl_3$): δ (ppm) 43.00. $^{13}C\{^1H\}$-NMR ($CDCl_3$): δ (ppm) 19.22 (s, CH_2), 25.59 (m [26]a, $N = 35.02$ Hz, PCH_2), 127.40, 129.08, 135.57 (s, C_6H_4), 128.28 (m, *m*-C_6H_5), 129.48 (s, *p*-C_6H_5), 133.10 (m, *o*-C_6H_5). FABMS; (*m*/*z*): 692.1 [M^+]. Anal. Found: C, 57.48; H, 4.95; Cl, 10.24; N, 4.04. Calc. for $C_{33}H_{34}Cl_2N_2P_2Ru$: C, 57.73; H, 4.62; Cl, 9.93; N, 3.59%.

4.2.6. 3L6

Complex **2** (500 mg, 0.50 mmol) was treated with $\mathbf{L_6}$ (0.067 g, 0.55 mmol) to give $\mathbf{3L_6}$. Yield 312 mg (88%) of a brown powder, m.p. 290 °C (dec.). ^{1}H-NMR ($CDCl_3$): δ (ppm) 1.86 (m, 2H, CH_2), 2.12 (br, 3H, CH_3), 2.79 (br, 4H, PCH_2), 4.25 (br, 4H, NH_2), 6.5–7.8 (m, 23H, C_6H_5, C_6H_3). $^{31}P\{^1H\}$-NMR ($CDCl_3$): δ (ppm) 42.70. $^{13}C\{^1H\}$-NMR ($CDCl_3$): δ (ppm) 19.29 (s, CH_2), 20.98 (s, CH_3), 25.66 (m [26]a, $N = 35.02$ Hz, PCH_2), 126.27, 127.92, 128.19, 128.81, 137.49, 139.91 (s, C_6H_3), 128.34 (m, *m*-C_6H_5), 129.43 (m, *p*-C_6H_5), 133.09 (m, *o*-C_6H_5). FABMS; (*m*/*z*): 706.1 [M^+]. Anal. Found: C, 57.79; H, 5.14; Cl, 10.03; N, 3.96. Calc. for

$C_{34}H_{36}Cl_2N_2P_2Ru$: C, 57.73; H, 4.68; Cl, 9.87; N, 3.89%.

4.2.7. $3L_7$

Complex **2** (500 mg, 0.50 mmol) was treated with $\mathbf{L_7}$ (0.116 g, 0.55 mmol) to give $\mathbf{3L_7}$. Yield 374 mg (96%) of a yellow powder, m.p. 318 °C (dec.). ^{1}H-NMR ($CDCl_3$): δ (ppm) 1.87 (m, 2H, CH_2), 2.76 (br, 4H, PCH_2), 3.00 (d, $^3J_{HH} = 8.80$ Hz, 2H, NH), 3.50 (m, 2H, CHN) 4.24 (d, $^3J_{HH} = 8.8$ Hz, 2H, NH), 6.64–7.73 (m, 23H, C_6H_5, C_6H_3). $^{31}P\{^1H\}$-NMR ($CDCl_3$): δ (ppm) 41.53. $^{13}C\{^1H\}$-NMR ($CDCl_3$): δ (ppm) 21.40 (s, CH_2), 28.20 (m [26]a, $N = 35.02$ Hz, PCH_2), 65.69 (s, HCN), 125.84, 128.24, 130.54, 131.23, 131.36, 131.95, 139.34, 148.62 (C_6H_5). FABMS; (m/z): 796.2 [M^+]. Anal. Found: C, 61.81; H, 5.31; Cl, 8.90; N, 3.52. Calc. for $C_{41}H_{42}Cl_2N_2P_2Ru$: C, 61.66; H, 5.17; Cl, 8.80; N, 3.21%.

4.2.8. $3L_8$

Complex **2** (500 mg, 0.5 mmol) was treated with $\mathbf{L_8}$ (0.116 g, 0.55 mmol) to give $\mathbf{3L_8}$. Yield 367 mg (94%) of a yellow powder, m.p. 318 °C (dec.). ^{1}H-NMR ($CDCl_3$): δ (ppm) 1.87 (m, 2H, CH_2), 2.75 (br, 4H, PCH_2), 3.05 (d, $^3J_{HH} = 8.8$ Hz, 2H, NH), 3.55 (m, 2H, CHN) 4.22 (d, $^3J_{HH} = 8.8$ Hz, 2H, NH), 6.5–7.8 (m, 23H, C_6H_5, C_6H_3). $^{31}P\{^1H\}$-NMR ($CDCl_3$): δ (ppm) 41.54. $^{13}C\{^1H\}$-NMR ($CDCl_3$): δ (ppm) 19.98 (s, CH_2), 26.57 (m [26]a, $N = 35.02$ Hz, PCH_2), 64.03 (s, HCN), 129.5, 130.2, 130.5, 131.0, 131.1, 131.5, 135.3, 142.7 (C_6H_5). FABMS; (m/z): 796.1 [M^+]. Anal. Found: C, 61.81; H, 5.31; Cl, 8.90; N, 3.52. Calc. for $C_{41}H_{42}Cl_2N_2P_2Ru$: C, 61.69; H, 5.10; Cl, 8.74; N, 3.76%.

4.2.9. $3L_9$

Complex **2** (500 mg, 0.50 mmol) was treated with $\mathbf{L_9}$ (0.046 ml, 0.55 mmol) to give $\mathbf{3L_9}$. Yield 317 mg (96%) of a yellow powder, m.p. 288 °C (dec.). ^{1}H-NMR ($CDCl_3$): δ (ppm) 1.52 (br, 6H, $N(CH_2)_3$, 1.84 (m, 2H, CH_2), 2.74, 2.81 (br, 8H, NH_2, PCH_2), 7.10–7.60 (m, 20H, C_6H_5). $^{31}P\{^1H\}$-NMR ($CDCl_3$): δ (ppm) 42.53. $^{13}C\{^1H\}$-NMR ($CDCl_3$): δ (ppm) 19.52 (s, PCH_2CH_2), 26.56 (m [26]a, $N = 35.02$ Hz, PCH_2), 29.47 (s, NCH_2CH_2), 40.29 (s, NCH_2), 128.06 (m [26]b, $N = 8.08$ Hz, m-C_6H_5), 129.4 (s, p-C_6H_5), 133.6 (br, o-C_6H_5), 136.4 (m, i-C_6H_5). FABMS; (m/z): 685.1 [M^+]. Anal. Found: C, 54.71; H, 5.51; Cl, 10.77; N, 4.25. Calc. for $C_{30}H_{36}Cl_2N_2P_2Ru$: C, 54.78; H, 5.17; Cl, 10.51; N, 3.99%.

4.2.10. $3L_{10}$

Complex **2** (500 mg, 0.5 mmol) was treated with $\mathbf{L_{10}}$ (0.065 ml, 0.55 mmol) to give $\mathbf{3L_{10}}$. Yield 291 mg (90%) of a yellow powder, m.p. 270 °C (dec.). ^{1}H-NMR ($CDCl_3$): δ (ppm) 0.75 (s, 6H, CH_3), 1.79 (m, 2H, CH_2), 2.50 (br, 4H, NCH_2), 2.73 (br, 8H, NH_2, PCH_2), 7.10–7.50 (m, 20H, C_6H_5). $^{31}P\{^1H\}$-NMR ($CDCl_3$): δ (ppm) 42.88. $^{13}C\{^1H\}$-NMR ($CDCl_3$): δ (ppm) 19.54 (s, CH_2), 24.79 (s, CH_3), 26.48 (m [26]a, $N = 32.02$ Hz, PCH_2), 34.45 (s, $C(CH_3)_2$), 49.97 (s, NCH_2), 128.13 (m [26]b, $N = 8.08$ Hz, m-C_6H_5), 129.24 (s, p-C_6H_5), 133.61 (br, o-C_6H_5), 136.24 (m, i-C_6H_5). FABMS; (m/z): 681.1 [M^+]. Anal. Found: C, 55.98; H, 5.87; Cl, 10.33; N, 4.08. Calc. for $C_{32}H_{40}Cl_2N_2P_2Ru$: C, 55.98; H, 5.48; Cl, 9.35; N, 3.64%.

4.2.11. $3L_{11}$

Complex **2** (500 mg, 0.5 mmol) was treated with $\mathbf{L_{11}}$ (0.066 ml, 0.55 mmol) to give $\mathbf{3L_{11}}$. Yield 291 mg (84%) of a yellow powder, m.p. 280 °C (dec.). ^{1}H-NMR ($CDCl_3$): δ (ppm) 0.35 (t, 3H, $^3J_{HH} = 7.5$ Hz, CH_3), 1.07 (m, 1H, NCH), 1.27 (m, 2H, CH_2CH_3), 1.48 (m, 2H, PCH_2CH_2), 1.54 (m, 2H, $CHCH_2$), 2.58 (s, 4H, NH_2), 2.95 (m, 6H, PCH_2, NCH_2), 7.10–7.50 (m, 20H, C_6H_5). $^{31}P\{^1H\}$-NMR ($CDCl_3$): δ (ppm) 42.24, 42.53 (AB pattern, $^2J_{PP} = 52.20$ Hz). $^{13}C\{^1H\}$-NMR ($CDCl_3$): δ (ppm) 9.70 (s, CH_3), 19.49 (s, PCH_2CH_2), 26.46 (2m, PCH_2), 33.15 (s, CH_2CH_3), 34.85 (s, $CHCH_2CH_2$), 40.50 (s, NCH_2), 52.35 (s, NCH), 127.83, 128.32, 129.37, 133.06, 134.04 (C_6H_5). FAB–MS; (m/z): 686.1 [M^+]. Anal. Found: C, 55.98; H, 5.87; Cl, 10.33; N, 4.08. Calc. for $C_{32}H_{40}Cl_2N_2P_2Ru$: C, 55.78; H, 5.76; Cl, 10.45; N, 4.07%.

4.2.12. $3L_{12}$

Complex **2** (500 mg, 0.5 mmol) was treated with $\mathbf{L_{12}}$ (0.057 ml, 0.55 mmol) to give $\mathbf{3L_{12}}$. Yield 219 mg (65%) of a yellow powder, m.p. 180 °C (dec.). ^{1}H-NMR ($CDCl_3$): δ (ppm) 0.78 (m, 4H, CH_2CH_2N), 1.18 (m, 4H, CH_2N), 1.59 (m, 4H, CH_2), 2.63, 2.74 (m, 8H, PCH_2, NH_2), 7.12–7.68 (m, 20H, C_6H_5). $^{31}P\{^1H\}$-NMR ($CDCl_3$): δ (ppm) 41.71. $^{13}C\{^1H\}$-NMR ($CDCl_3$): δ (ppm) 19.57 (s, CH_2), 26.87 (m [26]a, $N = 34.02$ Hz, PCH_2), 28.91 (s, CH_2CH_2N), 41.91 (s, NCH_2), 128.24, 129.43, 132.52, 133.93 (C_6H_5). FABMS; (m/z): 672.1 [M^+]. Anal. Found: C, 55.36; H, 5.69; Cl, 10.54; N, 4.17. Calc. for $C_{31}H_{38}Cl_2N_2P_2Ru$: C, 55.38; H, 5.47; Cl, 10.35; N, 3.84%.

4.3. General procedure for the catalytic studies

The respective diamine[bis(diphenylphosphino)propane]ruthenium(II) complexes $\mathbf{3L_1}$–$\mathbf{3L_{12}}$, (0.012 mmol) was placed in a 200 ml Schlenk tube and solid KOH (0.12 mmol) was added as a cocatalyst. The solid mixture was stirred and warmed during the evacuation process to remove oxygen and water. Subsequently the Schlenk tube was filled with argon and 20 ml of 2-propanol. The mixture was vigorously stirred, degassed by two freeze–thaw cycles, and then sonicated for 20–40 min (this is important to complete the dissolving of the catalyst and cocatalyst). A solution of *trans*-4-phenyl-3-

Table 3
Crystal data and structure refinement parameters for **3L$_1$**, **3L$_2$**, and **3L$_8$**

	3L$_1$	**3L$_2$**·CH_2Cl_2	**3L$_8$**
Empirical formula	$C_{29}H_{34}Cl_2N_2P_2Ru$	$C_{31}H_{38}Cl_4N_2P_2Ru$	$C_{41}H_{42}Cl_2N_2P_2Ru$
Formula weight	644.49	743.44	796.68
Crystal color	Yellow	Yellow	Orange
Crystal size (mm)	0.6 × 0.3 × 0.1	0.4 × 0.4 × 0.2	0.1 × 0.7 × 0.3
Crystal system, space group	Triclinic, $P\bar{1}$	Triclinic, $P\bar{1}$	Triclinic, $P1$
a (Å)	9.984(4)	10.0194(15)	10.2172(12)
b (Å)	12.519(7)	12.397(2)	13.4835(17)
c (Å)	13.476(8)	14.500(5)	14.3403(14)
α (°)	109.38(8)	82.51(3)	107.817(9)
β (°)	105.78(5)	74.387(18)	93.685(11)
γ (°)	105.15(4)	68.441(15)	102.019(12)
Z	2	2	2
μ (mm^{-1})	0.881	0.942	0.697
$F(000)$	660	760	820
θ Range (°)	2.27 to 27.52	2.25 to 27.50	2.06 to 27.50
Limiting indices, hkl	−12 to 12; −14 to 14; −17 to 17	−12 to 12; −16 to 15; −18 to 18	−12 to 13; −16 to 16; −18 to 18
Reflections collected/unique	12 434/6234 [$R_{int} = 0.0352$]	14 759/7384 [$R_{int} = 0.0225$]	16 453/16 453 [$R_{int} = 0.0000$]
Absorption correction	Empirical	None	Empirical
Max and min transmission	0.9169 and 0.7419	–	0.8335 and 0.5580
Data/restraints/parameters	6234/0/326	7384/0/363	16 453/3/866
Goodness-of-fit on F^2	1.083	1.042	1.047
Final R indices [$I > 2\sigma(I)$], R_1/wR_2	0.0318/0.0755	0.0290/0.0728	0.0276/0.0687
R indices (all data), R_1/wR_2	0.0366/0.0800	0.0326/0.0747	0.0315/0.0706
Absolute structure parameter	–	–	−0.021(18)
Extinction coefficient	0.0057(5)	0.0027(4)	0.0086(3)
Largest difference peak and hole (e $Å^{-3}$)	0.652 and −1.447	1.196 and −0.815	0.533 and −0.513

butene-2-one (12.0 mmol) in 40 ml of 2-propanol was subjected to a freeze–thaw cycle in a different 200 ml Schlenk tube and was added to the catalyst solution. Finally the reaction mixture was transferred to a pressure Schlenk tube which was pressurized with dihydrogen of 3 bar. The reaction mixture was vigorously stirred at 35 °C for 1 h. During the hydrogenation process samples were taken from the reaction mixture after the gas was been removed to control the conversion and turnover frequency. After this procedure the pressure Schlenk tube was pressurized again with hydrogen ($P_{H_2} = 3$ bar). The samples were inserted by a special glass syringe into a gas chromatograph and the kind of the reaction products was compared with authentic samples.

4.4. X-ray structural analyses for complexes 3L$_1$, 3L$_2$, and 3L$_8$

Crystallographic details of the structure determination of **3L$_1$**, **3L$_2$**, and **3L$_8$** are summarized in Table 3. Crystals of **3L$_1$**, **3L$_2$**, and **3L$_8$** were obtained by slow diffusion of diethyl ether into a dichloromethane solution of the complexes. A selected crystal was mounted on a Siemens P4 four-circle diffractometer by using a perfluorinated polyether (Riedel de Haen) as protecting agent. Graphite-monochromated Mo–K_α radiation ($\lambda = 0.71073$ Å) was used for the measurement of intensity data in the ω-scan mode at a temperature of 173(2) K. Cell parameters were determined from 35 to 50 automatically centered reflections. The intensity data was corrected for polarization and Lorentz effects. Structure solution and refinement were carried out using the Bruker SHELXTL package [27]. The structures were solved by Patterson synthesis, followed by identification of non-hydrogen atoms in successive Fourier maps. Refinement was carried out with full-matrix least-squares methods based on F^2, with anisotropic thermal parameters for all non-hydrogen atoms. Hydrogen atoms were included at calculated positions using a riding model with isotropic temperature factors equal to 1.2 times the U_{eq} value of the corresponding parent atom.

5. Supplementary material

Crystallographic data (excluding structure factors) for the structures in this paper have been deposited with the Cambridge Crystallographic Data Centre as supplementary publication number CCDC 190294, 190295, 190296. These data can be obtained free of charge from The Director, CCDC, 12 Union Road, Cambridge CB2 1EZ, UK (Fax: +44-1223-336033; e-mail:

deposit@ccdc.cam.ac.uk or http://www.ccdc.cam.ac.uk/conts/retrieving.html).

Acknowledgements

This work was supported by the Deutsche Forschungsgemeinschaft (Graduiertenkolleg 'Chemie in Interphasen' Grant. No. 441/2-01, Bonn-Bad Godesberg, Germany) and the Fonds der Chemischen Industrie.

References

[1] E. Lindner, I. Warad, K Eichele, H.A. Mayer, Inorg. Chim. Acta, in press.
[2] Reduction in Organic Synthesis: Recent Advances and Practical Applications: P.V. Ramachandran, H.C. Brown, ACS Symp. Ser. (1996) 641.
[3] A. Aramini, L. Brinchi, R. Germani, G. Savelli, Eur. J. Org. Chem. (2000) 1793.
[4] J.G. Handique, A. Purkayashtha, J.B. Baruah, J. Organomet. Chem. 620 (2001) 90.
[5] E.J. Corey, C.J. Helal, Tetrahedron Lett. 36 (1995) 9153.
[6] T. Ohkuma, H. Ooka, T. Ikariya, R. Noyori, J. Am. Chem. Soc. 117 (1995) 10417.
[7] T. Ohkuma, H. Ooka, S. Hashiguchi, T. Ikariya, R. Noyori, J. Am. Chem. Soc. 117 (1995) 2675.
[8] R. Noyori, T. Ohkuma, Angew. Chem. Int. Ed. 40 (2001) 40.
[9] H. Doucet, T. Ohkuma, K. Murata, T. Yokozawa, M. Kozawa, E. Katayama, A.F. England, T. Ikariya, R. Noyori, Angew. Chem. Int. Ed. 37 (1998) 1703.
[10] T. Ohkuma, M. Koizumi, H. Doucet, T. Pham, M. Kozawa, K. Murata, E. Katayama, T. Yokozawa, T. Ikariya, R. Noyori, J. Am. Chem. Soc. 120 (1998) 13529.
[11] T. Ohkuma, H. Takeno, Y. Honda, R. Noyori, Adv. Synth. Catal. 343 (2001) 369.
[12] M. Yamakawa, H. Ito, R. Noyori, J. Am. Chem. Soc. 122 (2000) 1466.
[13] R. Noyori, M. Yamakawa, S. Hashiguchi, J. Org. Chem. 66 (2001) 7931.
[14] O. Pämies, J.E. Bäckvall, Chem. Eur. J. 7 (2001) 5052.
[15] M.J. Burk, W. Hems, D. Herzberg, C. Malan, A. Zanotti-Gerosa, Org. Lett. 26 (2000) 4173.
[16] O.M. Akotsi, K. Metera, R.D. Reid, R. McDonald, S.H. Bergens, Chirality 12 (2000) 522.
[17] K. Abdur-Rashid, A.J. Lough, R.H. Morris, Organometallics 20 (2001) 1047.
[18] K. Abdur-Rashid, M. Faatz, A.J. Lough, R.H. Morris, J. Am. Chem. Soc. 123 (2001) 7473.
[19] C. Nachtigal, S. Al-Gharabli, K. Eichele, E. Lindner, H.A. Mayer, Organometallics 21 (2002) 105.
[20] E. Lindner, S. Al-Gharabli, H.A. Mayer, Inorg. Chim. Acta 334 (2002) 113.
[21] E. Lindner, A. Enderle, A. Baumann, J. Organomet. Chem. 558 (1998) 235.
[22] E. Lindner, T. Schneller, F. Auer, H.A. Mayer, Angew. Chem. Int. Ed. 38 (1999) 2154.
[23] M.M. Fontes, G. Oliva, L.C. Cordeiro, A. Batista, J. Coord. Chem. 30 (1993) 125.
[24] E. Lindner, I. Warad, K. Eichele, H.A. Mayer, unpublished results.
[25] T. Yamagishi, S. Ikeda, M. Yatagai, M. Yamaguchi, M. Hida, J. Chem. Soc. Perkin Trans. 1 (1988) 1787.
[26] A part of an AXX′ pattern: (a) $N = |^1J_{PC} + {}^3J_{PC}|$; (b) $N = |^3J_{PC} + {}^5J_{PC}|$.
[27] SHELXTL NT 5.10, Bruker AXS, Madison, WI, USA, 1998.